

Astro2020 Science White Paper

On The Unique Value of Spectroscopy in the Deep Ultraviolet for Galaxy Evolution Studies

Thematic Areas: Planetary Systems Star and Planet Formation
 Formation and Evolution of Compact Objects Cosmology and Fundamental Physics
 Stars and Stellar Evolution Resolved Stellar Populations and their Environments
 Galaxy Evolution Multi-Messenger Astronomy and Astrophysics

Principal Author:

Name: Todd M. Tripp

Institution: University of Massachusetts - Amherst

Email: tripp@astro.umass.edu

Phone:

Abstract:

The circumgalactic medium (CGM) is the keystone of galaxy evolution. The CGM mediates (1) the accretion of pristine intergalactic gas on the one hand, and (2) the AGN- and star formation-driven multiphase outflows of metal-enriched material on the other. These flows, and the physics of the baryons cycling in and out of galaxies, have a profound impact on the formation of stars, black hole interactions with host galaxies, and the physical conditions of the IGM in the vicinity of galaxies. They may play an important role in the transformation of galaxies. As such, the CGM was recognized by the Astro2010 science committees as a key topic of galaxy evolution. Significant observational and theoretical strides were made in CGM studies in the 2010–2020 period, but the topic is now growing explosively, and this will remain a central theme of galaxy evolution during the upcoming decade. This white paper focuses on a largely unexplored discovery space for CGM studies: the rich diagnostic information provided by absorption lines in the “deep” ultraviolet at rest wavelengths $< 912 \text{ \AA}$. Quantum physics places most of the resonance lines of a wide array of ions in this region, and these lines can be accessed by studying QSO absorption systems with sufficient redshift to bring these unique lines into the observable UV band. Unfortunately, this information cannot be exploited with ground-based telescopes because when the redshift is sufficient to redshift these lines into the optical, the Ly α forest causes blending that precludes detection and analysis of the lines. However, in the UV, lower redshift systems can be studied where the forest is thin enough to allow robust measurements. This paper shows some examples of UV observations of the deep UV and argues that it is important to begin developing a new space-based observatory with high-resolution spectroscopic capability.

The Challenges of Circumgalactic and Intergalactic Medium Studies. Ten years ago, the science panels of the Astro2010 Decadal Survey formulated a set of questions meant to capture the science priorities of astrophysics research in the 2010 – 2020 period. Multiple panels posed related questions about galaxy evolution including: (1) *What are the flows of matter and energy in the circumgalactic medium?* (2) *What controls the mass - energy - chemical cycles within galaxies?* [from the “Galactic Neighborhood” panel] (3) *How do cosmic structures form and evolve?* (4) *How do baryons cycle in and out of galaxies, and what do they do while they are there?* (5) *How do black holes grow, radiate, and influence their surroundings?* [“Galaxies Across Cosmic Time” panel]. The panel’s charge was to state questions “ripe for the answering”, but in 2019 these topics are hotter than ever. This is partly because good questions beget more good questions — good progress has been achieved on these questions, but the circumgalactic medium (CGM) exhibits many surprising characteristics, and recent studies suggest that the gas physics could be quite complicated — but this is also due in part to the stringent observational challenges presented by many parts of the “baryon cycle”.

One of the challenges is that intergalactic gas and inflowing/accreting circumgalactic gas typically has very low density. Likewise, as outflowing gas moves away from galaxies in various ways, it can expand/evolve into a very low-density entity. These low densities make CGM/IGM emission very difficult to detect, and with the notable exception of Ly α , few observational studies were able to map CGM emissions during the 2010 – 2020 decade. In recent years, the most powerful technique (i.e., with statistically useful samples and a variety of diagnostics) for probing the low-density IGM/CGM has been to study it in absorption, using both background quasars and “down-the-barrel” star clusters within galaxies as continuum sources (see, e.g., Tumlinson et al. 2017; Meiksin 2009 for reviews). With the advent of 30m-class ground-based telescopes, this technique will be a powerful tool in decades to come. However, as discussed below, due to the thick forest of H I Ly α lines that dominates (or, at high enough z , completely obliterates) the spectra of high- z objects observed from the ground, there is a huge amount of information that can only be accessed with ultraviolet spectrographs in space.

Why is the UV so important? The answer is that **quantum physics places the majority of the resonance-line CGM diagnostics at rest-frame wavelengths $\lambda_r \ll 1216 \text{ \AA}$, and many key lines are at $< 912 \text{ \AA}$** , hereafter referred to as the “deep UV”. Theory and observations indicate that the CGM is richly multiphase plasma (see Tumlinson et al. 2017, and references therein) including phases with a wide range of temperatures from the $\approx 10^4$ K “cool” gas to the $10^5 - 10^6$ “warm-hot” plasma and up to the $\gg 10^6$ K hot gas (for an observed example, see Tripp et al. 2011). To investigate all the important phases, it is necessary to push into the deep UV. This is illustrated in Figure 1(a), which shows detected resonance lines in the COS Absorption Survey of Baryons Harbors (CASBaH, see below and Tripp et al. 2011,2019), damped Ly α (DLA) absorbers, and high-velocity clouds (HVCs). In this plot, the rest wavelengths of resonance lines are shown with a vertical bar that is color-coded to indicate the ionization stage [see legend in Figure 1(b)], and the height of the bar indicates its expected strength (based on element abundance and atomic data; this does not account for ionization corrections, which of course depend on physical conditions). For clarity, Figure 1 does not show the plethora of UV H $_2$ lines that are also detected in some absorbers (see, e.g., Muzahid et al. 2015). Figure 1(a) shows: (1) as is well know, there is a dearth of resonance lines in the optical, mainly the Na I D, Ca II H&K, and very weak Ti II lines; Na D and Ca H&K are easily ionized, and all of these species are confused by dust depletion, (2) there are more lines in the UV at $1216 < \lambda_r < 3000 \text{ \AA}$ range used in the majority of QSO absorber

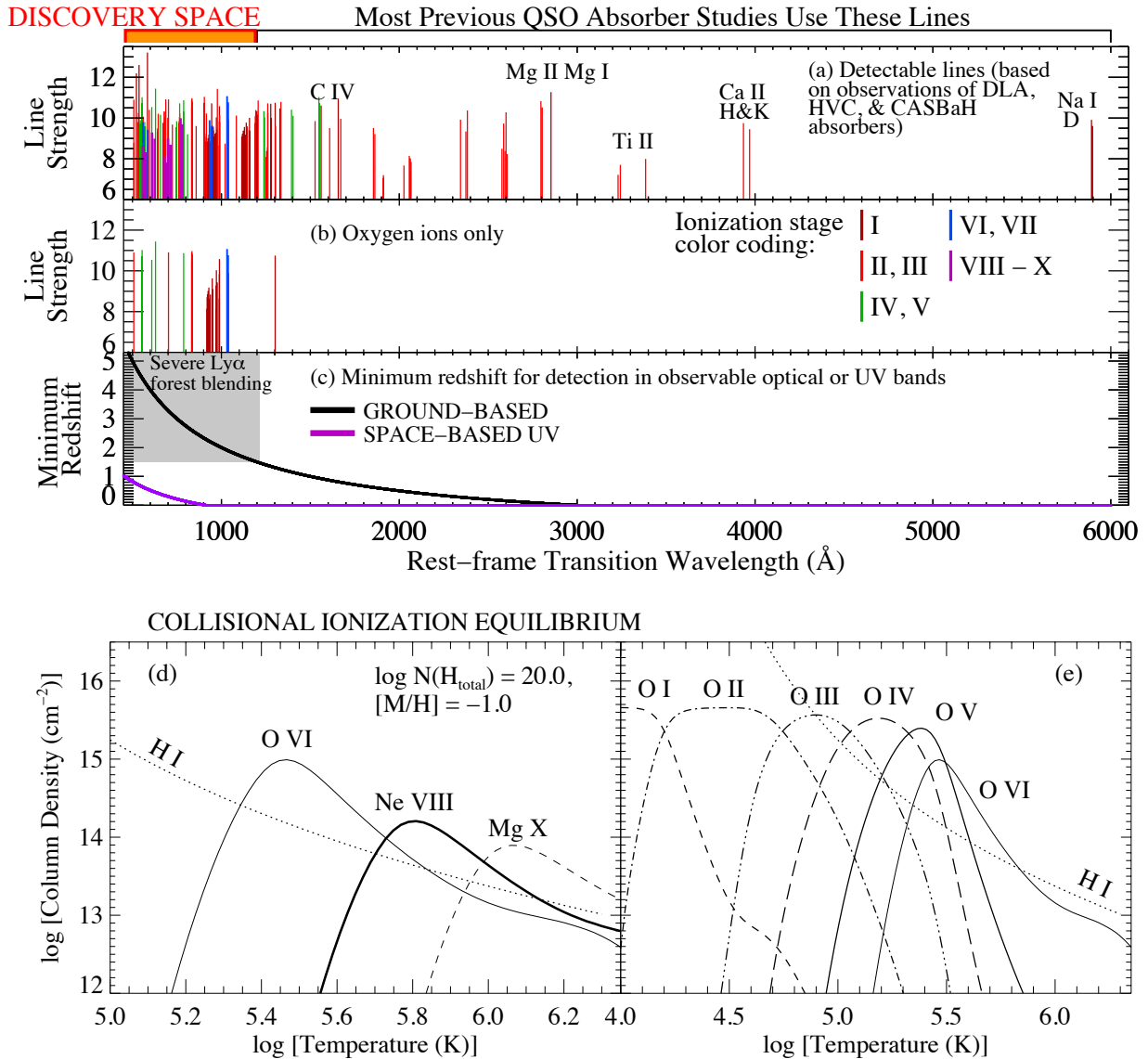


Figure 1: Illustration of the diagnostic power of the rest-frame ultraviolet band for low-density gas studies. The uppermost panel (a) shows the strength (= element abundance + atomic data) of resonance transitions of various ions vs. the rest wavelength λ_r of the line (each individual transition is shown with a vertical line; taller lines are stronger), color coded by ionization stage (see legend in middle panel b). The atomic data are from Verner et al. (1994,1996). These lines have been detected in CASBaH, DLA/sub-DLA, or HVC absorbers. THERE IS A TREMENDOUS AMOUNT OF INFORMATION IN THE (LARGELY UNTAPPED) DISCOVERY SPACE AT $\lambda_r \ll 912 \text{ \AA}$. Panel (b): same as a, but showing only oxygen ions. (c): Minimum redshift at which a transition at λ_r can be detected from the ground (black curve) or in space (purple curve). The gray box shows the redshift and λ_r region where blending with the Ly α forest becomes severe or prohibitive. Lowermost panels illustrate the abundance of interesting species vs. T in collisional ionization equilibrium (Gnat & Sternberg 2007), including warm-hot gas tracers (d) and oxygen ions (e).

studies, but the lines are still limited and are predominantly first and second ionization stages; very few diagnostics of intermediate- and high-ionization materials are accessible in this range (mainly Si III, Si IV, C IV, and occasionally Al III and N V), and (3) the vast majority of the good stuff is in the deep UV (see the orange bar labeled “DISCOVERY SPACE” in Figure 1).

The fact that many ions are not available in most QSO absorber studies introduces serious ambiguities into CGM investigations. Consider, for example, the most abundant element – oxygen. The detectable resonance lines of oxygen are shown in Figure 1(b). Typically, QSO absorber observations can cover the strong O I 1302.17 Å line (which is often not useful because it tends to be strongly saturated), the spin-changing O I 1355.60 Å transition (almost always too weak to detect in extragalactic absorbers), and possibly the O VI 1031.93, 1037.62 Å doublet (if it is not too corrupted by Ly α forest lines). Even if weaker O I lines can be pulled out of the Ly α forest, with only O I and maybe O VI, the ionization and physical nature of the gas is hugely uncertain. Of course, other elements often can be added to the analysis, but many issues still plague these studies (e.g., non-solar relative abundances, confusion from dust depletion, and most importantly, uncertain multiphase ionization structure). However, if a telescope+spectrograph can push into the discovery space in the deep UV, many of the oxygen ions (all ions between O I and O VI) can be reliably measured, along with analogous banks of, e.g., carbon (C I – C IV), nitrogen (N I – N V), neon (Ne II – Ne VIII), and sulfur (S I – S VI) ions (see examples in Figure 2, Tripp et al. 2011, 2019; Meiring et al. 2013; Hussain et al. 2015). With this information, we have found that the CGM absorbers often require at least three distinct phases (but are kinematically correlated, see below) that are probably not in pressure equilibrium (e.g., Haislmaier et al. 2019); these absorbers may be ephemeral and rapidly changing objects as predicted by some theoretical studies (e.g., Gronke & Peng 2018; Scheider et al. 2018). At any rate, exploiting information in the deep UV greatly expands and improves the constraints on the physical conditions, abundances, and physical implications of CGM absorbers, which in turn fills in missing pieces in our understanding of the baryon cycle and its implications regarding galaxy evolution. As an example of the additional constraints provided by the deep UV, we show the relative strengths warm-hot gas tracers and oxygen ions as a function of temperature (in CIE) in Figure 1 (d) and (e), respectively.

The ISM of the Milky Way totally attenuates all light shortward of the Lyman limit at $z = 0$, but we can observe extragalactic absorbers that are sufficiently redshifted to bring these lines into the observable bands. For example, if we wish to observe both lines of the Ne VIII 770.41, 780.32 Å doublet with *HST* (which has good sensitivity at observed wavelengths $\lambda_{\text{ob}} > 1150$ Å), we must study absorbers with $z_{\text{abs}} > 0.493$ so that $\lambda_{\text{ob}} = (1 + z_{\text{abs}})770.41 > 1150$ Å. With current technology, it is possible to build a high-resolution UV spectrograph with good sensitivity down to $\lambda_{\text{ob}} = 912$ Å (e.g., *FUSE*, Moos et al. 2000). Assuming good sensitivity down to $\lambda_{\text{ob}} = 912$ Å, Figure 1(c) shows the minimum redshift at which the lines in Figure 1(a,b) can be detected in space (purple line) compared to the minimum redshift at which these lines can be detected from the ground (assuming the ground can probe down to ≈ 3000 Å). This reveals why the deep-UV DISCOVERY SPACE cannot be accessed from the ground: to redshift the lines into the optical band, the absorber redshifts must so high that the lines will be located in the thick Ly α forest and will be extremely difficult (or impossible at higher redshifts) to reliably measure.

Proof of Concept: The COS Absorption Survey of Baryon Harbors. QSOs with bright continuum flux at $\lambda_{\text{ob}} \ll 912$ Å have been known for many years (e.g. Tripp et al. 1990, 1994), and with the deployment of the Cosmic Origins Spectrograph in 2009, it became possible to use these QSOs to observe absorption lines in the deep UV with good spectral resolution. Motivated by the

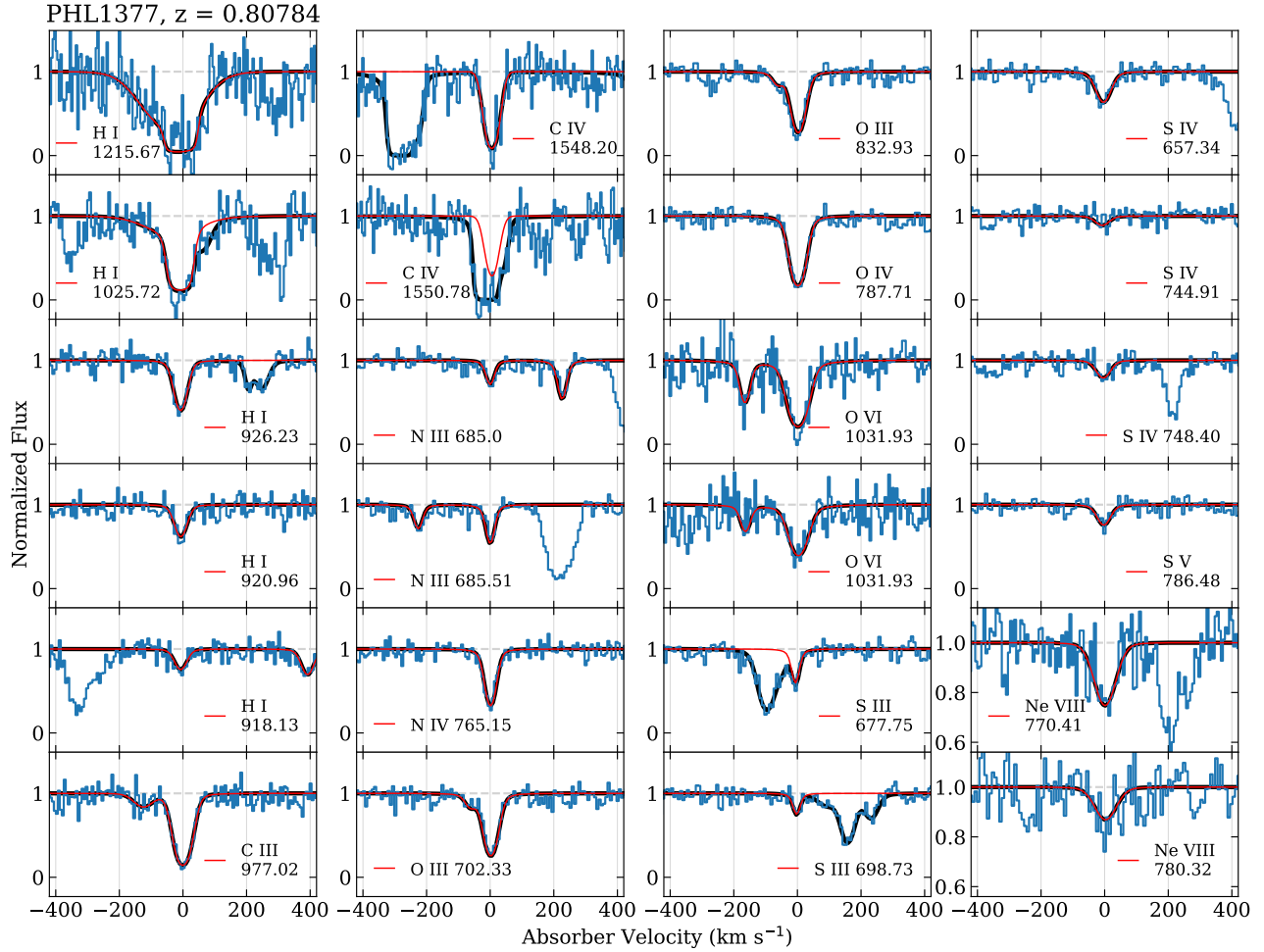


Figure 2: Example of the wide range of ions (including lines with rest wavelength $\lambda_r \ll 912 \text{ \AA}$) detected in a single absorption system at $z_{\text{abs}} = 0.80784$ in the spectrum of PHL1377: H I, C III, C IV, N III, N IV, O III, O IV, O VI, S III, S IV, S V, and Ne VIII (panels are labeled with the species and λ_r). The profiles (histograms) are continuum-normalized and plotted vs. velocity in the absorber frame ($v = 0 \text{ km s}^{-1}$ at $z_{\text{abs}} = 0.80784$). This absorber is affiliated with a galaxy at impact parameter = 103 kpc (spectroscopic $z_{\text{gal}} = 0.8077$) and thus probes the CGM near “cosmic noon”. Many of these species would not be observable without access to the deep UV ($< 912 \text{ \AA}$). Some of the lines are mildly blended; smooth black curves show full Voigt-profile fits (including blends with interloping lines), and the components at $z_{\text{abs}} = 0.80784$ only are indicated by red curves. Note the remarkable velocity alignment of these disparate ions ranging from H I (IP = 13.6 eV) up to Ne VIII (IP = 239.1 eV).

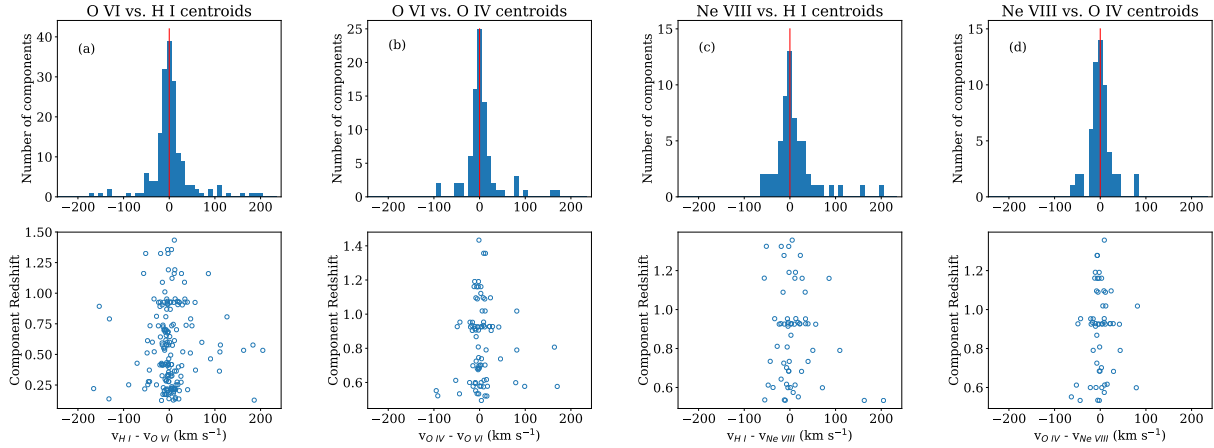


Figure 3: Velocity difference between the centroid of each detected O VI component ($v_{O\ VI}$) and the closest H I and O IV components of intervening CASBaH O VI absorbers (panels a and b). In each case, the upper panel shows the number with a given velocity difference (in 10 km s^{-1} bins), and the lower panel shows the velocity offset for the individual cases (open circles) vs. the component redshift (vertical axis). Panels c and d show the same quantities but comparing the velocity centroids of Ne VIII to those of the nearest H I and O IV components.

arguments above, the CASBaH program to observe the Tripp et al. (1994) QSOs was initiated, and this survey has beautifully demonstrated the potential of the deep UV. Figure 2 shows an example of the CASBaH data; the anticipated species are nicely detected in this system and many other absorbers, and the CASBaH database will be mined for many years. Some examples of the CASBaH results include detailed constraints on a massive outflow from a poststarburst/AGN galaxy (Tripp et al. 2011), identification of cold-accretion candidates (Ribaudo et al. 2011; Burchett et al. 2013), measurement of a bimodal metallicity distribution in a statistically useful sample of high- $N(\text{H I})$ absorbers (Lehner et al. 2013), discovery of strong nuclear AGN outflows (Muzahid et al. 2013), the CGM near cosmic noon (Bielby et al. 2019), and new results on O VI and Ne VIII in the halos of a large sample of galaxies (Burchett et al. 2019; Prochaska et al. 2019, Tripp et al. 2019). One fascinating CASBaH result is evident in Figure 2: even though the ionization potential of H I is only 13.6 eV, it is remarkably kinematically aligned (to within $5\text{--}10\text{ km s}^{-1}$) with O VI, Ne VIII, and everything in between. Since ionization of Ne VII to Ne VIII requires 207.3 eV, this alignment is downright bizarre and suggests that we have not fully comprehended the relevant physics of the CGM. This alignment is not unique to this absorber. Other systems (e.g., Tripp et al. 2011; Meiring et al. 2013) are similarly kinematically aligned, and as shown in Figure 3, most of the O I and Ne VIII absorbers are well aligned with H I and other lower ionization stages such as O IV (see Tripp et al. 2019 for details).

THE FUTURE? We have started to explore the deep-UV discovery space with *HST*, but we have only observed a handful of sightlines, and currently there are no plans to develop a spectroscopic UV telescope to follow after *HST*. *HST* is increasingly suffering serious hardware problems, and the unique deep-UV window will close soon. To understand how galaxy evolution is driven and regulated by the baryon cycle, the time has come to plan for the future of UV astronomy.

References

- Burchett, J. N., Tripp, T. M., Werk, J. K. et al. 2013, ApJ, 779, L17
- Burchett, J. N., Tripp, T. M., Prochaska, J. X. et al. 2019, ApJ, submitted (arXiv:1810.06560)
- Gnat, O., & Sternberg, A. 2007, ApJS, 168, 213
- Gronke, M. & Oh, S. P. 2018, MNRAS, 480, L111
- Haislmaier, K., Tripp, T. M., et al. MNRAS, submitted
- Hussain, T., Muzahid, S., Narayanan, A. et al. 2015, MNRAS, 446, 2444
- Lehner, N., Howk, J. C., Tripp, T. M. et al. 2013, ApJ, 770, 138
- Meiksin, A. 2009, RvMP, 81, 1405
- Meiring, J. D., Tripp, T. M., Werk, J. K. et al. 2013, ApJ, 767, 49
- Moos, H. W., Cash, W. C., Cowie, L. L. et al. 2000, ApJ, 538, 1
- Muzahid, S., Srianand, R., & Charlton, J. 2015, MNRAS, 448, 2840
- Muzahid, S., Srianand, R., Arav, N. et al. 2013, MNRAS, 431, 2885
- Prochaska, J. X., Burchett, J. N., Tripp, T. M. et al. 2019, ApJS, submitted
- Ribaldo, J., Lehner, N., Howk, J. C. et al. 2011, 743, 207
- Schneider, E. E., Robertson, B. E., & Thompson, T. A. 2018, ApJ, 862, 56
- Tripp, T. M., Bechtold, J., & Green, R. F. 1994, ApJ, 433, 533
- Tripp, T. M., Green, R. F., & Bechtold, J. 1990, ApJ, 364, L29
- Tripp, T. M., Meiring, J. D., Prochaska, J. X. et al. 2011, Science, 334, 952
- Tripp, T. M., et al. 2019, in preparation
- Tumlinson, J., Peebles, M. S., & Werk, J. K. 2017, ARAA, 55, 389
- Verner, D. A., Barthel, P. D., & Tytler, D. 1994, A&AS, 108, 287
- Verner, D. A., & Ferland, G. 1996, Atomic Data & Nuclear Data Tables, 64, 1